15 April 1995

ELSEVIER

OPTICS COMMUNICATIONS

Optics Communications 116 (1995) 109–115

Spontaneous phase symmetry breaking due to cavity detuning in a class-A bidirectional ring laser

D.V. Skryabin [a], A.G. Vladimirov [a], A.M. Radin [b]

[a] *Department of Quantum Electronics, Research Institute of Physics, St. Petersburg State University, 1 Ulianovskaya st., Petrodvorets, St. Petersburg, 198904, Russia*

[b] *Department of Applied Mathematics, Institute of Refrigeration, 9 Lomonosova st., St. Petersburg, 191002, Russia*

Received 15 July 1994; revised version received 22 December 1994

Abstract

We study the dynamics of a nonrotating class-A bidirectional ring laser with backscattering. A pair of new bistable time-dependent regimes with opposite values of beat frequency of counterpropagating waves is described. These regimes exist for certain cavity detunings.

1. Introduction

In the past three decades the bidirectional ring laser (BRL) has been attracting much attention of researchers, see Refs. [1–21]. It is well known that regimes with time-dependent intensities of the counterpropagating waves (CPWs) in nonrotating class-B BRL arise because of their coupling due to spatial modulation of the inversion in an active medium and due to backscattering from intracavity inhomogeneities [8–12]. Since the inversion relaxation time in a class-A BRL is small, the regimes with the time-dependent wave intensities can arise only in presence of backscattering [3–6,13–19]. Here we consider a nonrotating detuned class-A BRL with equal cavity eigenfrequencies and losses of the CPWs. Pump parameters and backscattering coefficients of the CPWs are assumed to be equal. The equations describing this model are invariant under the transformation

$$(E_+, E_-) \to (E_-, E_+) . \qquad (1)$$

Here E_+ (E_-) is the electric field envelope of the clockwise (counterclockwise) wave. The symmetry property (1) reflects the equivalence of clockwise and counterclockwise directions of propagation.

The three kinds of regimes of a class-A BRL were described earlier. (i) The regimes with time-independent and approximately equal intensities of the CPWs. Below they will be named the standing wave regimes. (ii) The regimes with time-independent and unequal intensities of the CPWs. Below they will be named the running wave regimes. (iii) The time-dependent regimes characterized by the antiphase oscillations of the CPW intensities and the oscillations of the phase difference of the CPWs $\mu(t) = \arg(E_+) - \arg(E_-)$. Note that in a nonrotating BRL only such regimes for which the beat frequency

$$\Delta = \frac{1}{T}\int_0^T \frac{\mathrm{d}\mu(t)}{\mathrm{d}t}\,\mathrm{d}t , \qquad (2)$$

is equal to zero, were earlier described. Here T is the period of the CPW intensities oscillations. The first two

SSDI 0030-4018(95)00050-X

regimes (i) and (ii) exist in lasers with and without backscattering, see Refs. [2–5,12–21], whereas the third regime (iii) was caused by backscattering, see Refs. [3–6,14–19]. The antiphase oscillations of the CPW intensities may be interpreted as frequency splitting of two standing waves, sin kz and cos kz, see Refs. [16–18]. This splitting is proportional to the absolute value of backscattering coefficients, see Refs. [3,4,17–19].

The running wave regimes (ii) are usual for a single-isotope HeNe laser tuned to the small vicinity of the line center [3,21,22] and for a dye laser [15,18]. The transition from a standing wave regime to a running wave regime is an example of spontaneous symmetry breaking. The two running wave regimes exist simultaneously due to the symmetry property (1). One of these two regimes corresponds to $|E_+|^2 > |E_-|^2$, and the other corresponds to $|E_+|^2 < |E_-|^2$. The spontaneous symmetry breaking phenomenon was recently reported for a laser operating in several transverse modes, see Refs. [23–25]. When some controlling parameter is changed a mode with cylindrical symmetry bifurcates into two modes that are bistable and do not possess this symmetry [23]. As it was shown in Ref. [26], the symmetry breaking bifurcation in a system of two identical coupled oscillators can be followed by the bifurcations leading to chaotic behavior.

This paper is organized as follows. In section 2 we describe the model of a bidirectional class-A laser. In section 3 we present the results of numerical analysis of steady-state and periodic solutions. We show that a pair of stable periodic solutions with nonzero beat frequencies exist for certain cavity detunings. For one of these solutions the beat frequency is $\Delta = 2\pi/T$ and for the other $\Delta = -2\pi/T$. The transition to the regime with nonzero beat frequency in a BRL for which clockwise and counterclockwise directions are equivalent we have named a spontaneous phase symmetry breaking. In section 4 the concluding remarks are given.

2. Laser equations

In the weak-field approximation the equations describing a single-frequency operation of a class-A BRL with backscattering are (see Refs. [1–7])

$$
\begin{aligned}
(\partial_t + \gamma_c)\tilde{E}_+ &= \eta[\alpha - \beta|\tilde{E}_+|^2 - \vartheta|\tilde{E}_-|^2]\tilde{E}_+ \\
&\quad + iR\tilde{E}_- \exp(i\psi) , \\
(\partial_t + \gamma_c)\tilde{E}_- &= \eta[\alpha - \beta|\tilde{E}_-|^2 - \vartheta|\tilde{E}_+|^2]\tilde{E}_- \\
&\quad + iR\tilde{E}_+ \exp(i\psi) ,
\end{aligned} \tag{3}
$$

where $\tilde{E}_\pm$ are the slowly-varying electric field envelopes of the CPWs; η is the amplification at the line center; γ_c is the cavity decay rate; R and ψ are the amplitude and the phase of backscattering. α, β, and ϑ are the complex coefficients depending on the detuning, inhomogeneous and/or homogeneous linewidths and on the inversion relaxation time of an active medium

$$\alpha = \alpha' + i\alpha'', \quad \beta = \beta' + i\beta'', \quad \vartheta = \vartheta' + i\vartheta'' ,$$

where β' and ϑ' are the self- and cross-saturation coefficients of the CPWs.

The total field in the BRL is

$$
\begin{aligned}
E_{\rm tot} = [\,&|\tilde{E}_+| \exp(i\mu_+(t) + ikz) \\
&+ |\tilde{E}_-| \exp(i\mu_-(t) - ikz)] \exp(-i\omega t) + \text{c.c.} ,
\end{aligned}
$$

where ω is the optical frequency, z is the coordinate along the cavity axis, k is the wave number and $\mu_\pm$ are the slowly varying phases of the CPWs.

Let $R \neq 0$. Then, passing to the variables amplitude-phase in the set (3) we obtain

$$
\begin{aligned}
\partial_\tau|E_+| &= [A - |E_+|^2 - |E_-|^2 - S\cos\phi(|E_+|^2 \\
&\quad - |E_-|^2)]|E_+| + \sin(\mu - \psi)|E_-| , \\
\partial_\tau|E_-| &= [A - |E_+|^2 - |E_-|^2 + S\cos\phi(|E_+|^2 \\
&\quad - |E_-|^2)]|E_-| - \sin(\mu + \psi)|E_+| , \\
\partial_\tau\mu &= -2S\sin\phi(|E_+|^2 - |E_-|^2) \\
&\quad + \frac{|E_-|}{|E_+|}\cos(\psi - \mu) - \frac{|E_+|}{|E_-|}\cos(\psi + \mu) ,
\end{aligned} \tag{4}
$$

where

$$
\tau = tR, \quad A = \frac{\eta\alpha' - \gamma_c}{R}, \quad S\exp(i\phi) = \frac{\beta - \vartheta}{\beta' + \vartheta'},
$$
$$
|E_\pm| = \sqrt{\frac{(\beta' + \vartheta')\eta}{2R}}|\tilde{E}_\pm|, \quad \mu = \mu_+ - \mu_- . \tag{5}
$$

The parameter A is the ratio of the pump parameter and the backscattering amplitude and it can be varied in a wide range in experimental conditions. The parameter

ψ describes the phase of backscattering. If $\psi=\pi M$ with integer M, the coupling of the CPWs is conservative and if $\psi=\pi(1/2+M)$ it is dissipative, see Ref. [18]. The parameter ψ may be easily controlled in an experiment with the help of two outer mirrors, see Refs. [1,19]. The parameters S and ϕ are real. If $\phi\in[\pi/2, 3\pi/2]$ then $\beta'<\vartheta'$. This relation holds for a single-isotope HeNe BRL tuned to a small vicinity of the line center [3,21] and for a dye BRL [17]. If $\phi\in[0, \pi/2]$, $[3\pi/2, 2\pi]$ then $\beta'>\vartheta'$. This relation holds for a single-isotope HeNe BRL operating far from the line center and for a HeNe BRL with two-isotope mixture [3]. For example, when the cavity detuning in a single-isotope HeNe laser is changed from $+\infty$ to $-\infty$, the parameter ϕ changes from 2π to 0.

Note, that for $\beta=1$, $\vartheta=2$, Eqs. (1) are transformed into the equations that were derived in Ref. [27] to describe the operation of a CO_2 laser in two transverse modes. Thus, the results presented here can be applied to study the dynamics of this laser.

For the variables amplitude-phase (5) the symmetry property (1) can be rewritten as

$$(|E_+|, |E_-|, \mu)\rightarrow(|E_-|, |E_+|, -\mu)\ . \tag{6}$$

Since Eqs. (4) are invariant under the transformation $\mu\rightarrow\mu+2\pi$, their phase space is a cylinder. Therefore, Eqs. (4) may possess two kinds of limit cycles differing in their topological properties. The limit cycle of the first kind can be continuously shrunk to a point on a cylinder. For such cycles the phase difference μ oscillates around certain mean value and, hence, the beat frequency (2) is equal to zero. The limit cycles of the second kind cannot be shrunk to a point on a cylinder. These cycles correspond to regimes with nonzero beat frequency of the CPWs. We have found that Eqs. (4) possess stable limit cycles of both kinds (see below). Some further comments concerning these two kinds of limit cycles are given in the Appendix.

3. Steady-state and time-dependent regimes

Eqs. (6) have seven branches of steady-state solutions describing the regimes with time-independent intensities of the CPWs. The trivial solution $|E_+|=|E_-|=0$ with undefined μ corresponds to the laser off. It is unstable for $A>-|\sin\psi|$.

There are two branches of steady-state solutions, SW1 and SW2, corresponding to the standing wave regimes:

$$\text{SW1:}\quad |E_+|^2=|E_-|^2=A-\sin\psi,\quad \mu=2\pi N\ ,$$
$$\text{SW2:}\quad |E_+|^2=|E_-|^2=A+\sin\psi,$$
$$\mu=\pi(2N+1)\ , \tag{7}$$

where N is integer. The transitions from one standing wave to another and the accompanying π-jumps of the phase difference μ were investigated in Refs. [17,19].

There are four branches of the steady-state solutions (RW1, RW2, RW3, and RW4) corresponding to the running wave regimes. Explicit expressions for these solutions and some results concerning bifurcations of steady-states are given in the Appendix.

The bifurcation diagram in (A, ϕ) plane for $S=0.7$ and $\psi=\pi/3$ is presented in Fig. 1. This diagram was calculated using the programs LINLBF and LINBAS, see Ref. [28]. The first of them is designed for calculation of steady-state bifurcations in a system of ordinary differential equations. It is based on the Newton's method applied to solve a set of nonlinear algebraic equations and on a specially designed algorithm used to trace bifurcation curve in parameter space. The second program, LINBAS, is similar to LINLBF, but it

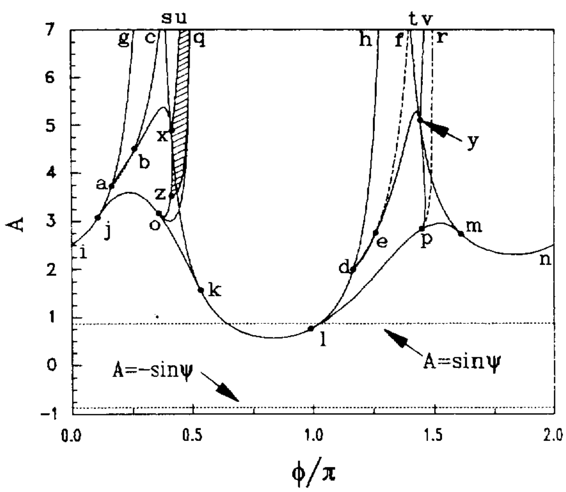

Fig. 1. Bifurcation diagram for Eqs. (4). $S=0.7$, $\psi=\pi/3$. The stable limit cycle LC1 exists in the region *cbxuc*. The stable limit cycles LC3 and LC4 exist in the region *uxzoqu*. The beat frequencies of the CPWs are nonzero for LC3 and LC4 in the dashed region.

deals with fixed points of the Poincaré section, which correspond to periodic solutions.

The solution SW1 (SW2) exists for $A > \sin\psi$ ($A > -\sin\psi$). SW1 is stable in the region *gabcg*. SW1 undergoes supercritical (subcritical) pitchfork bifurcation on the lines *ij* and *mn* (*jag* and *myt*). It undergoes supercritical (subcritical) Hopf bifurcation on the line *bc* (*ab*). The stable limit cycle LC1 emerges from SW1 on the line *bc*. The CPW intensities and phase difference versus time for LC1 are shown in Figs. 2a, b. LC1 exists in the region *cbxuc*. LC1 disappears on the line *bx* (*ux*) in the heteroclinic orbit connecting RW3 and RW4 (in the homoclinic figure eight orbit with a center in SW2). The unstable limit cycle arising on the line *ab* exists in a very small region near *ab*. SW2 is stable outside the curve *sxkldef* and above the line $A = -\sin\psi$. SW2 undergoes supercritical (subcritical) pitchfork bifurcation on *kl* (*sxk* and *ldh*), and supercritical (subcritical) Hopf bifurcation on *de* (*ef*). The stable limit cycle LC2 arising on the line *de* exists in an extremely narrow domain. We do not show it in Fig. 1. Dependencies of the CPW intensities and phase difference on the time for LC2 are similar to those for LC1. The unstable limit cycle arising via subcritical Hopf bifurcation on the line *ef* exists in the region *feyvf*. For both the limit cycles, LC1 and LC2, arising via Hopf bifurcations of the standing waves SW1 and SW2, the beat frequencies of the CPWs are equal to zero, i.e., $\Delta = 0$.

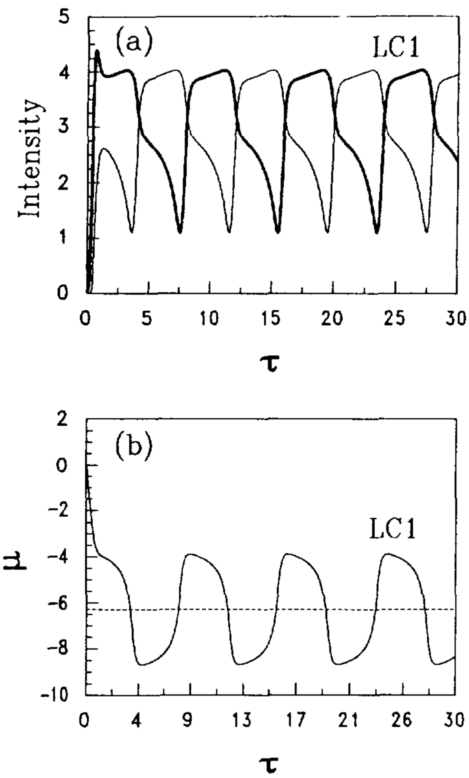

Fig. 2. Time evolution of the CPW intensities and their phase difference for a limit cycle LC1. $A = 6$, $S = 0.7$, $\psi = \pi/3$, $\phi = 0.41\pi$. (a) Thick (thin) line corresponds to $|E_+|^2$ ($|E_-|^2$). (b) Solid line corresponds to $\mu(\tau)$, dashed line $\mu = -2\pi$ indicates the unstable steady-state SW1.

The running wave solutions, RW1 and RW2 (RW3 and RW4), arise after supercritical (subcritical) pitchfork bifurcation of SW1 and SW2. RW3 and RW4 exist in the domains *gajokxsg* and *hdlpmyth*, and they are always unstable. RW1 and RW2 exist above the curve *ijoklpmn*. They are stable in the domain *qoklprq*. RW3 (RW4) and RW1 (RW2) merge and disappear via a saddle-node bifurcation on the lines *jok* and *lpm*. Due to the symmetry property (6) RW1 and RW2 undergo all their bifurcations simultaneously. Supercritical (subcritical) Hopf bifurcations of RW1 and RW2 occur on the curve *oq* (*pr*). The unstable limit cycles arising on the line *pr* exist in the region *vyprv*. The stable limit cycles LC3 and LC4 arising after supercritical Hopf bifurcations of RW1 and RW2 exist in the domain *uxoqu*. LC3 and LC4 vanish on the line *ux* in the homoclinic figure eight orbit with a center in SW2. After this homoclinic bifurcation the limit cycle LC1 arises. LC3 (LC4) vanishes on the line *xo* where the steady-state RW3 (RW4) has a homoclinic orbit. The limit cycles LC3 and LC4 emerging via a Hopf bifurcation on the line *oq* and via a homoclinic bifurcation on the line *oz* correspond to zero beat frequency, $\Delta = 0$. LC3 (LC4) touches the subspace $|E_+| = 0$ ($|E_-| = 0$) of the phase space on the line starting at the point *z* and asymptotically approaching to the line *oq*, see Fig. 1. This tangency results in changing of the limit cycle topology and it is accompanied by the beat frequency jump from zero to $2\pi/T$ ($-2\pi/T$) for LC3 (LC4), see Fig. 4. Similar mechanism of the beat frequency appearance was described in Refs. [7,20] for a rotating class-A BRL. The regimes with nonzero beat frequency exist in the dashed region in Fig. 1. They are shown in Fig. 3. This region is bounded from the left by the homoclinic bifurcation lines *zx* and *xu*.

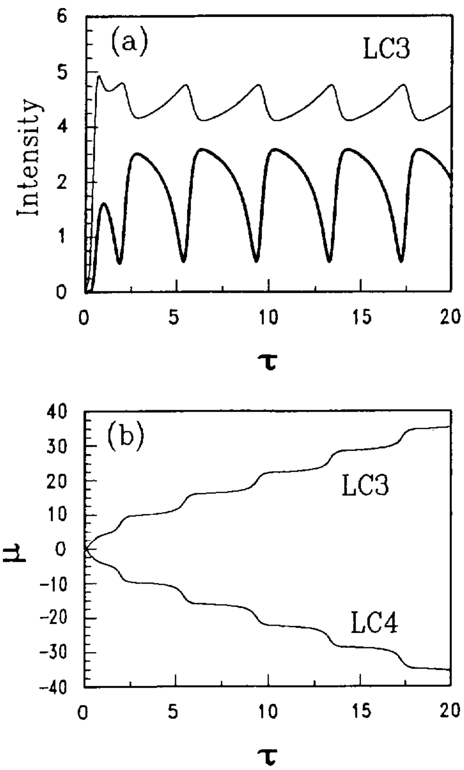

Fig. 3. Time evolution of the CPWs intensities and their phase difference for the limit cycles LC3 and LC4. $A=6$, $S=0.7$, $\psi=\pi/3$, $\phi=0.45\pi$. (a) Thick (thin) line corresponds to $|E_+|^2$ ($|E_-|^2$) for a laser operating in LC3 regime. For LC4 regime the thick and the thin line must be interchanged. (b) $\mu(\tau)$ for the limit cycles LC3 and LC4.

4. Conclusion

We have shown that a nonrotating class-A bidirectional laser with backscattering can demonstrate time-dependent regimes with nonzero beat frequency of the counter-propagating waves, see Figs. 3b, 4, even if the clockwise and counterclockwise directions of propagation are equivalent. Regimes with nonzero beat frequency were described earlier only in a laser with cavity phase nonreciprocity, see Refs. [1,2,5,7,20].

Christian and Mandel [14], carried out experimental measurements of the dependence of the counterpropagating wave intensities on the detuning in a single-isotope HeNe ring laser with a scattering diaphragm. For small pump parameters they observed a standing wave operation for any detuning and for greater pumps – a running wave regime. The running waves had

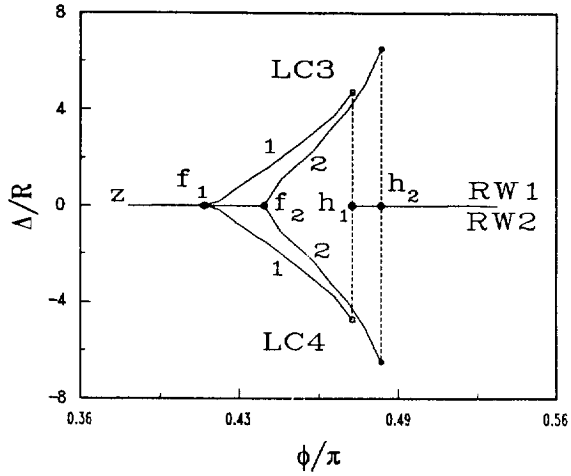

Fig. 4. Beat frequency as a function of the parameter ϕ. Curves 1 (curves 2) correspond to $A=4.5$ ($A=6$). $S=0.7$, $\psi=\pi/3$. Homoclinic bifurcation occurs at the point f_1 (f_2). At the point h_1 (h_2) the limit cycle LC3 (LC4) touches the subspace $|E_+|=0$ ($|E_-|=0$). For $A=4.5$ the steady-state solution SW2 is stable on the line zf_1. For $A=6$ the limit cycle LC1 is stable on the line zf_2.

undergone instability and a regime with time-dependent intensities of the counterpropagating waves arose in a definite interval of detunings. This interval was situated on the one side of the amplification line, see Fig. 9a in Ref. [14]. Our results are in agreement with this experiment. We obtained a stable standing wave operation for small pumps and running waves or time-dependent regimes for greater pumps. The stable time-dependent solutions exist on the one side of the amplification line (see Fig. 1, where $\phi=\pi$ corresponds to the laser operating at the line center).

Appendix

Let us make the following change of variables in the laser equations (4)

$$x_1=|E_+|^2-|E_-|^2,\quad x_2=-2|E_-||E_+|\sin\mu,$$
$$x_3=2|E_-||E_+|\cos\mu,$$
$$x_4=|E_+|^2+|E_-|^2. \tag{A.1}$$

The variables (A.1) were used in Refs. [5,7] and they are suitable for analytic and numeric investigation of the laser dynamics. In the new variables Eqs. (4) take the form

$$\partial_{\tau'} x = \begin{pmatrix} A & -\cos\psi & 0 & 0 \\ \cos\psi & A & 0 & 0 \\ 0 & 0 & A & -\sin\psi \\ 0 & 0 & -\sin\psi & A \end{pmatrix} x - \begin{pmatrix} x_1 x_4 (1+S\cos\phi) \\ x_2 x_4 - x_1 x_3 S \sin\phi \\ x_3 x_4 + x_1 x_2 S \sin\phi \\ x_4^2 + x_1^2 S \cos\phi \end{pmatrix} . \tag{A.2}$$

Here $x=(x_1, x_2, x_3, x_4)^{\mathrm{T}}$ and $\tau'=2\tau$. Using the relation

$$0=x_1^2+x_2^2+x_3^2-x_4^2 \equiv \Phi(x) , \tag{A.3}$$

which can be easily obtained from (A.1), the dimension of Eqs. (A.2) can be reduced from four to three. Here $\Phi(x)=0$ is a hypercone. For Eqs. (A.2) the symmetry property (1), (6) is transformed into

$$(x_1, x_2, x_3, x_4) \to (-x_1, -x_2, x_3, x_4) . \tag{A.4}$$

The standing wave solutions (7) can be rewritten as

$$\text{SW1:} \quad x_1=0,\ x_2=0,\ x_3=A-\sin\psi,\ x_4=A-\sin\psi ,$$

$$\text{SW2:} \quad x_1=0,\ x_2=0,\ x_3=-A-\sin\psi ,$$

$$x_4=A+\sin\psi . \tag{A.5}$$

The stability of SW1 and SW2 on the hypercone $\Phi(x)=0$ is determined by the roots λ_i of the characteristic polynomial

$$(\lambda+A\pm\sin\psi)(\lambda^2-\mu_1\lambda+\mu_2)=0 . \tag{A.6}$$

Here

$$\mu_1=\pm 2\sin\psi+S(A\pm\sin\psi)\cos\phi ,$$

$$\mu_2=1\pm S(A\pm\sin\psi)\sin(\phi-\psi) . \tag{A.7}$$

The lower (upper) signs in (A.6) and (A.7) corresponds to SW1 (SW2). The equation $A=\sin\psi$ ($A=-\sin\psi$) defines the threshold for SW1 (SW2). The conditions $\mu_1=0$ and $\mu_2>0$ correspond to a Hopf bifurcation. This bifurcation occurs on the line *abc* for SW1 and on the line *def* for SW2, see Fig. 1. The condition $\mu_2=0$ corresponds to a pitchfork bifurcation. It occurs on the lines *ijag* and *nmyt* for SW1 and on the line *sxkldh* for SW2, see Fig. 1. When both the conditions $\mu_1=0$ and $\mu_2=0$ are satisfied simultaneously we have a codimension-two bifurcation point of the Takens-Bogdanov type [29]. The Takens-Bogdanov bifurcation point of the solution SW1 (SW2) is labeled $a(d)$ in Fig. 1.

The running wave solutions RW1 and RW3 are given by

$$x_1=\sqrt{\frac{Ax_4-\sin\psi\, x_3-x_4^2}{S\cos\phi}} ,$$

$$x_2=\frac{x_1[A-x_4(1+S\cos\phi)]}{\cos\psi} ,$$

$$x_3=\frac{\sin(\phi-\psi)}{U}\left(\cos\psi-\frac{A}{2U}(AS\pm\sqrt{Z})\right) ,$$

$$x_4=\frac{A+\cos\psi\,(AS\pm\sqrt{Z})/2U}{1+S\cos\phi} , \tag{A.8}$$

here

$$U=\cos(\phi-\psi)-S\sin\phi\sin(\phi-\psi) ,$$

$$Z=A^2S^2-4U(1+S\cos\phi)\cos(\phi-\psi) . \tag{A.9}$$

The sign plus (minus) in (A.8) corresponds to RW1 (RW3). The solution RW2 (RW4) can be obtained from RW1 (RW3) using the symmetry property (A.4). Saddle-node bifurcation of RW1 and RW3 (RW2 and RW4) occurs when $Z=0$, see lines *jok* and *lpm* in Fig. 1. Hopf bifurcations of the running wave solutions, homoclinic and heteroclinic bifurcations were calculated numerically, see section 3. The Takens-Bogdanov bifurcation point of RW1 (RW2) is labeled o (p) in Fig. 1.

As it was already mentioned, in section 2 the laser model considered can exhibit two kinds of limit cycles. In the phase space of Eqs. (A.2) they can be distinguished by their projections on the plane (x_2, x_3). (i) If the projection of a limit cycle on this plane surrounds the origin $x_2=x_3=0$ then the phase difference of the CPWs μ is unbounded in time and the beat frequency is $\Delta=\pm 2\pi/T$, see (2). Here T is the period of the limit cycle and the sign plus (minus) corresponds to a counterclockwise (clockwise) round trip. (ii) If the projection of a limit cycle does not surround the origin then μ is a bounded function of time and $\Delta=0$. The limit cycles LC1 and LC2 described in section 3 are always the cycles of the second kind (ii). The limit cycles LC3 and LC4 are the cycles of the first kind (i) in the dashed region in Fig. 1. For a rotating laser limit cycles of both kinds were described in Ref. [7]. In Ref. [30] two different kinds of limit cycles were found in the Maxwell-Bloch equations with an additional term describing an injected field. It was shown that limit cycle projection on the plane real-imaginary part of the field amplitude can surround or not surround the origin.

References

[1] Yu.L. Klimontovich, V.N. Kuryatov and P.S. Landa, Zh. Eksp. Teor. Fiz. 51 (1966) 3.
[2] L.N. Menegozzi and W.E. Lamb Jr., Phys. Rev. A 8 (1973) 2103.
[3] Yu.L. Klimontovich, P.S. Landa and E.G. Lariontsev, Zh. Eksp. Teor. Fiz. 52 (1967) 1617.
[4] S.A. Bidichov, P.S. Landa and E.G. Lariontsev, Radiotekhnika i Elektronika. 15 (1970) 529.
[5] Wave and stochastic phenomena in lasers, ed. Yu.L. Klimontovich (Moskow, Nauka, 1974).
[6] F. Aronowitz, Appl. Optics 1 (1972) 405.
[7] C. Etrich, P. Mandel, R.C. Neelen, R.J.C. Spreeuw and J.P. Woerdman, Phys. Rev. A 46 (1992) 525.
[8] E.G. Klochan, L.S. Kornienko, N.V. Kravtsov, E.G. Lariontsev and A.N. Shelaev, Zh. Eksp. Teor. Fiz. 65 (1973) 1344.
[9] N.V. Kravtsov, E.G. Lariontsev and A.N. Shelaev, Laser Physics 3 (1993) 21.
[10] H. Zeglache, P. Mandel, N.B. Abraham, L.M. Hoffer, G.L. Lippi and T. Mello, Phys. Rev. A 37 (1988) 470.
[11] P.A. Khandokhin and Ya.I. Khanin, J. Opt. Soc. Am. B 2 (1985) 226.
[12] K. Staliunas, M.F.H. Tarroja and C.O. Weiss, Optics Comm. 109 (1993) 69.
[13] V.N. Lisitsyn and B.I. Troshin, Opt. Spektrosk. 22 (1967) 666.
[14] W.R. Christian and L. Mandel, Phys. Rev. A 34 (1986) 3932; 36 (1987) 1510.
[15] D. Külke, Acta Phys. Pol. A 61 (1982) 547.
[16] F.C. Cheng, Optics Comm. 82 (1991) 45; F.C. Cheng, Phys. Rev. A 45 (1992) 5220.
[17] R.C. Neelen, R.J.C. Spreeuw, E.R. Eliel and J.P. Woerdman, J. Opt. Soc. Am. B 8 (1991) 959.
[18] R.J.C. Spreeuw, R.C. Neelen, N.J. van Druten, E.R. Eliel and J.P. Woerdman, Phys. Rev. A 42 (1990) 4315.
[19] T.H. Chyba, Phys. Rev. A 40 (1989) 6327.
[20] T.H. Chyba, Optics Comm. 76 (1990) 395; T.H. Chyba, in: Laser Noise, ed. R. Roy, Proc. SPIE 1376 (1990) 132.
[21] I.A. Andronova, I.L. Bershtein and I.A. Markelov, Kvantovaya Elektron. 1 (1974) 645.
[22] J.B. Hambinne and M. Sargent III, Phys. Rev. A 13 (1976) 797.
[23] C. Tamm and C.O. Weiss, J. Opt. Soc. Am. B 7 (1990) 1034.
[24] M. Brambilla, F. Battipede, L.A. Lugiato, V. Penna, F. Prati, C. Tamm and C.O. Weiss, Phys. Rev. A 43 (1991) 5090.
[25] M. Brambilla, M. Catteneo, L.A. Lugiato, R. Pirovano, F. Prati, A.J. Kent, G.L. Oppo, A.B. Coates, C.O. Weiss, C. Green, E.J. D'Angelo and J.R. Tredicce, Phys. Rev. A 49 (1994) 1452.
[26] S.D. Glysin, in: Qualitative and approximate methods in analysis of operator equations, Yaroslavl (1986) pp. 112–127; Proc. third Intern. Conf. on Nonlinear oscillations in mechanical systems, Nyzhny Novgorod (1993) p. 55.
[27] R.López-Ruiz, G.B. Mindlin, C. Pérez-Garcia and J.R. Tredicce, Phys. Rev. A 49 (1994) 4916.
[28] A.I. Khibnik, in: Algorithms and programs in FORTRAN: materials for the mathematical support of computers, Vol. 5. (Special National Information Center, Scientific Center for Biological Research, Pushino, 1979).
[29] J. Guckenheimer and P. Holmes, Nonlinear oscillations, dynamical systems, and bifurcations of vector fields (Springer, Berlin, 1983).
[30] P.A. Braza, Optics Comm. 103 (1993) 95.